IOP Publishing Journal of Micromechanics and Microengineering

J. Micromech. Microeng. **25** (2015) 015011 (10pp) doi:10.1088/0960-1317/25/1/015011

Lift-off of large-scale ultrathin nanomembranes

Joshua J Miller[1], Robert N Carter[1], Kelly B McNabb[1], Jon-Paul S DesOrmeaux[2], Christopher C Striemer[2], Joshua D Winans[3] and Thomas R Gaborski[1]

[1] Department of Biomedical Engineering, Rochester Institute of Technology, 160 Lomb Memorial Drive, Rochester, NY 14623, USA
[2] SiMPore Inc., 150 Lucius Gordon Drive, West Henrietta, NY 14586, USA
[3] Department of Biomedical Engineering, University of Rochester, Rochester, NY 14627, USA

E-mail: trgbme@rit.edu

Received 16 October 2014, revised 11 November 2014
Accepted for publication 25 November 2014
Published 30 December 2014

Abstract

Ultrathin silicon-based nanomembranes hold significant promise for advancements in applications ranging from separations to tissue engineering. Widespread application of these membranes has been hindered by their small active area, which typically ranges from square micrometers to square millimeters. These membranes are typically supported on silicon chips as small windows as a result of a time-consuming through-wafer etch process. This approach results in a relatively low active area and can be challenging to integrate into devices because of the rigid silicon support. In this paper, a lift-off approach is demonstrated wherein the membrane is supported by a polymeric scaffold and separated from the wafer to enable fabrication of membrane sheets (>75 cm^2) with >80% active area. The wafer-scale lift-off process is demonstrated with 50 nm thick microporous and nanoporous silicon nitride (SiN) membranes. Release of large-scale SiN membranes is accomplished with both wet and dry lift-off techniques. The dry approach uses XeF_2 gas to etch a sacrificial silicon film, while the wet etch uses buffered oxide etchant to remove a silicon dioxide sacrificial layer. Finally, it is demonstrated that lift-off membranes have excellent optical properties and can be used to support cell culture on a conventional scale.

Keywords: nanomembrane, silicon, lift-off, mesenchymal stem cell

S Online supplementary data available from stacks.iop.org/JMM/25/015011

(Some figures may appear in colour only in the online journal)

1. Introduction

Nanomembranes have the ability to advance a variety of fields including separations, energy production, sensing and medicine as well as advance fundamental understanding of nanoscale phenomena [1–8]. Ultrathin (<100 nm) membranes have a number of benefits over conventional membranes including orders of magnitude greater diffusive and hydraulic permeability, minimal surface area and improved optical quality [2, 9]. Many of these ultrathin membranes are silicon-based due to precise control over thickness, pore size and surface functionalization [10]. Compared to ultrathin organic and polymeric membranes, Si-based membranes typically have greater mechanical stability and chemical resistance.

One of the first demonstrations of enhanced separations using an ultrathin membrane was with porous nanocrystalline silicon (pnc-Si) in 2007 [10]. These membranes have demonstrated precise separation of proteins and nanoparticles, while supporting as much as 1 bar of differential pressure [11]. Pnc-Si membranes have also been used for cell culture, electro-osmotic pumping, lab-on-a-chip as well as testing the feasibility of portable hemodialysis [9, 12–14]. Recently, pnc-Si has been used to template an ultrathin nanoporous silicon nitride (SiN) membrane [15]. This work has led to

 © 2015 IOP Publishing Ltd Printed in the UK

increased pore size control and mechanical strength over pnc-Si.

In the development of *in vitro* tissue models, polymeric track-etched (TE) membranes have been used for years in part due to their defined micrometer-scale pore sizes and through-pore structure. This pore geometry is ideal for investigations of directed cellular transmigration. Unfortunately, TE membranes are approximately 10 μm thick and have poor optical clarity. The thickness minimizes opportunities for cell–cell contact in co-culture studies and the optical qualities hinder live cell imaging. Efforts to overcome these issues were put forth by the Shuler laboratory in the development of an *in vitro* blood brain barrier (BBB) model using microporous SiN membranes [16, 17]. Our group has also used ultrathin Si-based microporous membranes to investigate adipose-derived stem cell (ADSC) differentiation in co-culture models with human endothelial cells [18]. Like most Si-based membranes, active areas were limited to a couple of square millimeters, which yielded approximately one thousand cells, a scale too small for ultimate clinical and therapeutic uses [19].

Other applications of silicon-based membranes thus far have also been limited to proof of concept experiments and lab-on-a-chip devices due to membrane areas ranging from square micrometers to square millimeters. There has been significant promise of utilizing the existing massive semiconductor infrastructure to scale up nanomembrane manufacturing, but it has not yet materialized. Furthermore, these nanomembranes are supported on silicon chips, which require a time-consuming process of through-wafer etching to expose small windows of suspended membrane [10, 20]. This form factor can be challenging to integrate into devices because of the rigid nature of silicon. While efforts have been made to develop processes that create supporting frames within the silicon wafer, they require complex front-side to back-side lithography alignment and multiple etch steps that consume the silicon wafer [21]. Another approach using thin film scaffolding of SiN over pnc-Si membranes has increased active area [14], but not by the orders of magnitude required for many real-world applications.

To address the issues with the present form factor of silicon-based nanomembranes, we propose using a lift-off approach wherein the membrane is supported by a micro-scale polymeric scaffold and separated from the wafer in a through-pore etch to produce free-standing sheets of large area membranes. This approach based in part on the methods used routinely in MEMS (micro-electro-mechanical systems) micromachining involving sacrificial layers. One example is to blanket coat a patterned photoresist layer or stencil on a target substrate followed by stripping the stencil along with the material it supports to leave behind the desired patterned material on the substrate [22, 23]. Another example is the fabrication of free-standing structures by under-etching sacrificial layers of silicon [24, 25]. In all these cases, the free-standing device is still connected to the silicon substrate by an attachment point. In the present study however, the nanomembrane is completely removed from the silicon wafer substrate. This lift-off from the rigid silicon wafer results in a flexible, yet robust ultrathin membrane, opening the door to additional applications and manufacturing integration methods. Thus, this method simultaneously increases the active area by many orders of magnitude, eliminates the through-wafer etch, and removes the rigid wafer support. We explore two different lift-off approaches utilizing XeF_2 and buffered oxide etchant (BOE), each with a different sacrificial film. Most of the effort in this study is focused on developing the lift-off methods using 50 nm thick microporous SiN, which enables much easier visual inspection of the through-pore etch progress using optical microscopy. Still, preliminary tests also demonstrate successful lift-off of nanoporous SiN membranes. Finally, cell culture on the ultrathin lift-off membranes is demonstrated on a scale never before achieved with a silicon-based membrane.

2. Methods

2.1. Sacrificial layer and SiN membrane

All tests were performed with standard ø150 mm silicon wafers ($\langle 1\,0\,0\rangle$ orientation, single-side-polished, 700 μm thick). The first step was application of the sacrificial layer of either silicon or silicon dioxide for the through-pore etch process. For the XeF_2 etch, an etch stop layer of silicon dioxide was applied to the wafer prior to applying the sacrificial Si film. The oxide layer (100 nm) was thermally grown on the wafer (Bruce Tube Furnace) at 1100 °C with oxygen (ambient pressure) at a growth rate of 1.7 nm min^{-1}. This thickness was chosen largely because its deep blue color provides good visual contrast tracking of the through-pore etch during the lift-off process with optical microscopy. The sacrificial poly-silicon layer was deposited as a 1 μm thick layer with low-pressure chemical vapor deposition (LP-CVD, ASM LPCVD System). Deposition was done at 650 °C using SiH_4 at 40 Pa resulting in a 20 nm min^{-1} growth rate. The BOE etch requires a sacrificial layer of silicon dioxide. Three different forms of the oxide, which were each 150 nm thick, were studied. The first is thermal oxide grown as described above. The second is PE-CVD of tetraethylorthosilicate (TEOS) using an Applied Materials P5000 tool. The third method is RF magnetron sputtering (AJA ATC 2000-V), wherein SiO_2 is sputtered from two ø7.5 cm silicon dioxide targets (300 W each) at a chamber pressure of 0.7 Pa with a 20 : 1 Ar : O_2 gas flow ratio, yielding a deposition rate of 1.5 nm min^{-1}.

Following the deposition of the sacrificial layers, the wafers were cleaned in standard RCA process and then coated with a 50 nm thick layer of low stress SiN (Rogue Valley Microdevices, Oregon) using LP-CVD. The film stress of the silicon-rich SiN layer was nominally 250 MPa, tensile. For the microporous membranes, the SiN film was patterned (ø2 μm, hexagonal close-packed pores with 6 μm pitch) using photolithography. First, the wafers were coated with a primer (HMDS, Dow) on a CEE manual spin-coater. After drying the primer for 60 s at 150 °C, a positive photoresist layer (Microposit® S1813, Shipley) was spin coated and then dried for 60 s at 130 °C. Patterning was done using a G-line stepper (6000 Series DSW Wafer Stepper) capable of 5 × pattern reduction. The wafers were exposed to 150 mJ cm^{-2} and then developed using MF-CD-26 (Shipley) for 120 s. The pore pattern was

then transferred to the 50 nm thick SiN layer using reactive ion etching (RIE, DryTek 482 Quad Etcher) at 13 Pa using a mixture of SF_6 and Ar flowing at a 1 : 2 ratio and 125 W of RF power. Etching through the 50 nm film was accomplished in 45 s. Following this, the photoresist was stripped in a 10 min piranha bath soak followed by deionized water rinse.

Nanoporous SiN membranes were also fabricated by transferring the nanoporous pattern of pnc-Si into a SiN film [15]. Briefly, the 50 nm thick LP-CVD nitride layer was sputter-coated with a 40 nm layer of amorphous silicon followed by a 20 nm layer of silicon dioxide using RF-sputtering in the same AJA ATC 2000-V system used to create the sacrificial oxide layer described above. The wafer was then exposed to a rapid thermal anneal process (RTP; Surface Science Integration Solaris 150) where it was heated in nitrogen at 100 °C s^{-1} to 1050 °C and held for 60 s. This process causes the amorphous silicon to crystallize and form the nanocrystalline silicon (pnc-Si) layer. The 20 nm oxide was then removed in a 45 s strip using 10 : 1 BOE. This leaves a nanoporous silicon mask on top of the solid SiN layer. Nanoporous transfer to the nitride layer was then accomplished using RIE in the Drytek 482 Quad Etcher with the following conditions: 200 W power for 70 s at 10 Pa, CHF_3, CF_4, O_2 and Ar were flowed at 50 sccm, 10 sccm, 5 sccm and 100 sccm, respectively. The CF_4 acts as the primary etchant, while the addition of hydrogen from CHF_3 provides selectivity toward the nitride over silicon. Oxygen and argon are added to increase the anisotropy of the etch.

2.2. Support scaffold

The scaffold was formed from SU-8 series 3010 (MicroChem), a negative photoresist. This material was chosen because of its favorable properties regarding adhesion, thickness and film stress. Starting with suggestions from the manufacturer and found on MEMS webpages the following procedure was developed for our application. Approximately 12 ml of the resist was deposited in the center of a stationary wafer using a disposable pipet. The spin coating program was: 500 RPM for 10 s with 500 RPM s^{-1} ramp followed by 3000 RPM for 45 s with 300 RPM s^{-1} ramp, resulting in a film that is approximately 10 μm thick. The coated wafer was then dried on a hotplate at 95 °C for 150 s. Exposure was done on a Suss MA150 Contact Aligner where the wafer was exposed to a broadband spectrum (no filter) to obtain at least 200 mJ cm^{-2} exposure. The post-exposure cure was in two steps: first 60 s at 65 °C and then 150 s at 95 °C. Development was done with SU-8 developer (MicroChem) for 180 s with mild agitation. The wafer was then rinsed with isopropyl alcohol (IPA) for 10 s on each side using a rinse bottle, dipped in a water bath for 60 s, and then rinsed again with IPA. A final, hard bake was done for 150 s at 120 °C. The wafer was cut into rectangular sections to define the size of membrane to be lifted off.

2.3. XeF_2 lift-off etch

It was found that the XeF_2 etch time could be reduced four-fold by removing the native oxide on the sacrificial silicon layer with a brief etch in BOE just prior to the XeF_2 etch. The wafer sections were dipped in the BOE long enough for the entire membrane surface to be wetted. The XeF_2 etch was performed in a Xetch® e1 Series Etcher (Xactix) using 60 s pulses of 0.4 kPa XeF_2. Control tests showed that the XeF_2 gas was consumed within this timeframe. The progress of through-pore etch was measured using optical microscopy, and it was determined that complete membrane lift-off could be achieved after three pulses with a 2.5 × 2.5 cm sample.

2.4. BOE lift-off etch

Wafer sections were etched in a 10 : 1 BOE solution with surfactant (J T Baker) for times ranging from a two minutes to several tens of minutes. The through film or vertical etch rate was determined for each of the oxide types by measuring the film thickness using a spectrophotometer (Nanometrics Model 200) of samples removed at different time intervals from the etch solution. The lateral etch rates were measured using optical micrographs taken of samples with a nanoporous SiN layer and SU-8 scaffold that were removed at different time intervals from the etch solution. The etch progress under the SU-8 struts can be readily determined visually due to the clear color change from blue to white when the sacrificial silicon dioxide layer is removed. In lift-off tests, the samples became visually cloudy as the lateral etch removed the underlying oxide layer, and once the entire surface of the sample appeared this way, the sample was transferred to a water bath using wafer tweezers. The membrane would float on top of the water and could be removed with a plastic sieve. The etch rate of the SiN layer in 10 : 1 BOE solution was calculated by measuring the thickness of the SiN layer using a spectrophotometer before and after a 35 min etch.

2.5. Cell culture on lift-off membranes

A section of lift-off membrane was suspended above a glass coverslip with a 1 mm thick silicone gasket. Prior to incubation, the membrane was sterilized by washing in 70% ethanol/water for 30 min and then dried in an oven at 60 °C for several hours. Feasibility of dry cycle autoclave sterilization (121 °C for 15 min) was also performed successfully. The membrane was incubated with a 1% w/v basement membrane protein mixture (Geltrex, Life Technologies) in 1 × PBS (phosphate-buffered saline) for 30 min at room temperature and then aspirated prior to seeding cells. Commercially available human ADSCs were purchased from Life Technologies (Carlsbad, CA) and used after their third passage. They were cultured in non-differentiating proliferation media for four days on the top side of the membrane. Cells were fixed (4% formaldehyde) and permeabilized (0.1% Triton X-100 in PBS) and then stained with 4′,6-diamidino-2-phenylindole (DAPI, blue) and Fluoroscein-Phalloidin (green) following manufacturer's recommendations (Life Technologies, Carlsbad, CA). Images were collected at 10 × and 20 × on a Leica DMI3000

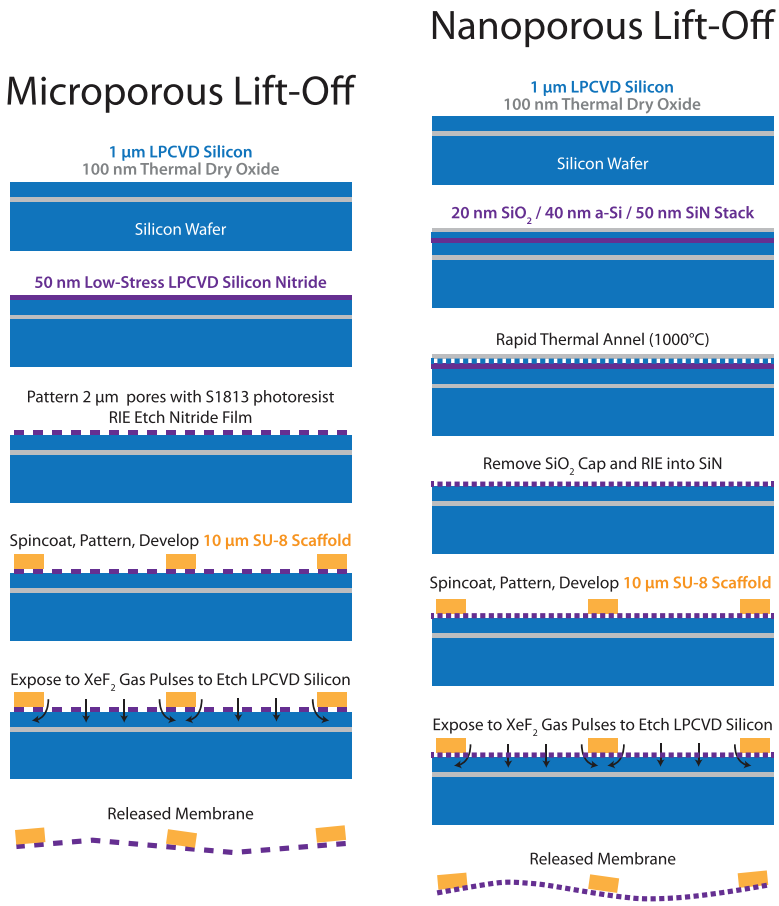

Figure 1. A process flow diagram for lift-off of micro- and nano-porous SiN membranes using XeF_2.

(Buffalo Grove, IL) inverted stage microscope and Leica DFC345 FX camera in phase contrast and fluorescence.

3. Results and discussion

3.1. Membrane deposition and scaffold patterning

The general approach based on a dry etch with XeF_2 that was used to perform lift-off of both microporous and nanoporous nitride membranes is outlined in figure 1. For both cases, a sacrificial layer of poly-silicon was deposited on a thermal oxide etch stop layer. This sacrificial layer was subsequently removed in a through-pore etch to free the nitride membrane from the wafer substrate. The SiN layer was deposited using LP-CVD with a silicon-rich stoichiometry to form a low stress film. These films were then processed to form the micro- or nano-pores according to the steps outlined in figure 1. The micro-pores (ø2μm, close-packed pattern with 6μm pitch) were patterned using standard photolithography and RIE. The nanoporous membrane preparation method is described in detail elsewhere [15] and will be briefly summarized here. The membrane is fabricated by first forming a nanoporous silicon (pnc-Si) layer on top of the solid nitride film and then using the pnc-Si as a mask to transfer its nanopores to the nitride though a RIE process as outlined in figure 1.

Also, common to both methods is the application of a polymeric scaffold prior to the lift-off etch. The purpose of the scaffold is to provide mechanical support for the membrane once it is separated from the wafer substrate. It is formed from an epoxy resin photoresist (SU-8, 3000-series, MicroChem) that is spin coated to an approximate thickness of 10μm and patterned with 100μm square openings and 10μm wide struts. The factors involved in choosing these dimensions are three-fold: maximize the open area of the porous membrane, provide adequate mechanical support for the SiN membrane once separated from the wafer substrate, and minimize the under-membrane etch distance required during lift-off. These scaffold dimensions provide slightly better than 80% open area for the membrane. Regarding mechanical support, the open window span of the scaffold is based on our previous experience with silicon-based membranes of this thickness that are supported by silicon chips after through-wafer etching to expose windows of the nanomembrane material. Generally, if the minor dimension is maintained at ~100μm, this provides membrane windows with sufficient strength to withstand 1 bar of differential pressure without failure [10]. The width of the struts was limited to 10μm to provide both a readily patterned dimension though contact lithography and to minimize the lateral distance required in the lift-off etch. The SU-8 features cover the micro-pores in the SiN membrane, thus for struts of

width w, the maximum under-etch distance reaches $\sqrt{2w^2}/2$ (i.e. 1/2 the diagonal of the strut intersections). Therefore, the strut width was chosen in part to be on the same order as the spacing of the micro-pores.

We also explored a wet etch-based lift-off process involving BOE solution and a silicon dioxide sacrificial layer. In general, the process flow is the same as in figure 1 except that the SiN membranes were prepared on a silicon dioxide film instead of a poly-silicon one. Of the two etch methods explored in this study, the XeF_2 showed superior performance over the BOE method toward lift-off of SiN membranes. This is largely due to the relative etch rates and selectivities of the sacrificial layers versus the SiN membrane for the two methods. XeF_2 etches Si at approximately 200–400 nm min^{-1} and is essentially zero for SiN [26, 27], thus having an essentially infinite selectivity toward the sacrificial layer. In contrast, while BOE etches the sacrificial silicon dioxide very rapidly at rates of 60–160 nm min^{-1}, it does show a measurable rate for SiN of 0.20 nm min^{-1} (based on control tests for 10 : 1 BOE with surfactant). Thus, despite having a large selectivity toward the sacrificial layer, the BOE etch process will clearly result in loss of some of the nitride membrane. Additionally, dry etch processes are preferable when working with ultrathin porous membranes, because one avoids the challenges regarding surface tension and capillary forces associated with wet etch procedures. The motivation for developing the BOE etch method is to enable potential future lift-off of silicon membranes (such as pnc-Si). Additionally, the wet etch process tends to be more amenable to scale up.

The 3000-series SU-8 was chosen because of its lower film stress (compared with 2000-series) and good adhesion to SiN. Since the purpose of the polymer scaffold is to provide mechanical support for the 50 nm thick SiN membrane once it is separated from the wafer, it is critical that the residual stress properties of the scaffold be compatible with the membrane. If upon separation from the wafer, relaxation of the scaffold's stress exerts a significant force, then the film will either buckle or rupture. From a standpoint of using the membrane as a cell culture support, it is desirable that the membrane be free of wrinkles to simplify cell seeding and imaging. The SiN film used here has a tensile stress of approximately 250 MPa, which implies that it will shrink by approximately 0.1% upon release, assuming a Young's modulus of 255 GPa for low stress SiN films [28, 29]. Therefore, it is desirable that the SU-8 grid displays a similar level of strain upon release from the silicon wafer. To examine this, a small section of the SU-8 scaffold (approximately 0.5 × 2 cm) was lifted off from a bare silicon wafer (i.e. no underlying SiN membrane) using a XeF_2 dry etch and compared for dimensional change relative to the mask used to pattern it. Measuring over the 2 cm span, it was found that the scaffold's grid had shrunk by 0.23%. This value is both small and close to that predicted for the SiN film, so it is predicted that the SU-8 scaffold should not cause deformations of the lifted-off membrane, which is consistent with our observations described below.

3.2. XeF_2 lift-off

The reaction associated with XeF_2 etching of silicon is

$$2XeF_2 + Si \rightarrow SiF_4 + 2Xe\,. \quad (1)$$

A pulsed gas system by Xactix was used that exposes the sample to pulses of XeF_2 gas from an expansion chamber that is charged by sublimation of XeF_2 crystals to a pressure of 0.6 kPa.

Dry etch results using XeF_2 with the microporous membrane are illustrated in figure 2. The oxide layer underneath the sacrificial silicon layer has a deep blue color at the 100 nm thickness used for these tests, which makes it convenient to discriminate between etched and unetched regions. In figure 2(*a*), the pores in the SiN membrane appear dark blue because the dry etch has exposed the underlying oxide layer. The etch zone extending under the SiN membrane appears as light gray rings and is in high contrast to the red region where the sacrificial silicon is still present under the SiN. The release of a 2.5 × 2.5 cm sample can be achieved after just three pulses. From figure 2(*b*), it can be seen that the SU-8 struts clearly block the micro-pores resulting in longer under-etch distance in those regions. The progression of the under-etch can be visualized after each XeF_2 pulse (online supplemental figure S1 (stacks.iop.org/JMM/25/015011)). It was found that all of the etchant gas was consumed within the first 60 s of sample exposure to the XeF_2 pulse. This was determined by exposing different samples to a single pulse for times ranging from 60 to 300 s before purging the etch chamber with nitrogen. Subsequent measurements of the amount of silicon that was etched (diameter of the light gray ring surrounding the ø2 μm pores) showed that it did not increase beyond that seen for a 60 s etch time.

Once the procedure had been optimized for lifting off these smaller samples, a sample with dimensions of 7.5 × 10 cm was tested to determine the efficacy of the technique for membranes of a scale that is more practical for larger scale applications. Visible separation of the membrane was observed starting at pulse 36 and appeared to span the entire area by pulse 42. The sample was exposed to an additional 10 pulses prior to removing from the etch chamber to ensure complete separation prior to attempting lift-off. Lift-off was accomplished by first gently pulling one corner of the membrane from the wafer using tweezers until about half of the area was separated (figure 2(*e*)), and then switching to pulling with a gloved hand to completely separate the membrane from the wafer substrate (figure 2(*f*)). A video of the membrane release from the silicon substrate is available in the online supplementary material (stacks.iop.org/JMM/25/015011).

The sequential nature of the XeF_2 pulses can be seen not only in the optical images during the etching process, but also in SEM micrographs (figure 3). For large lift-off samples that require many etch pulses, it is possible to see concentric ring features around the pores on the bottom surface of the membrane (figures 3(*a*) and (*b*)). These rings merge between pores at the corners of the SU-8 scaffold as would be predicted. The released membrane shows significant flexibility when curled

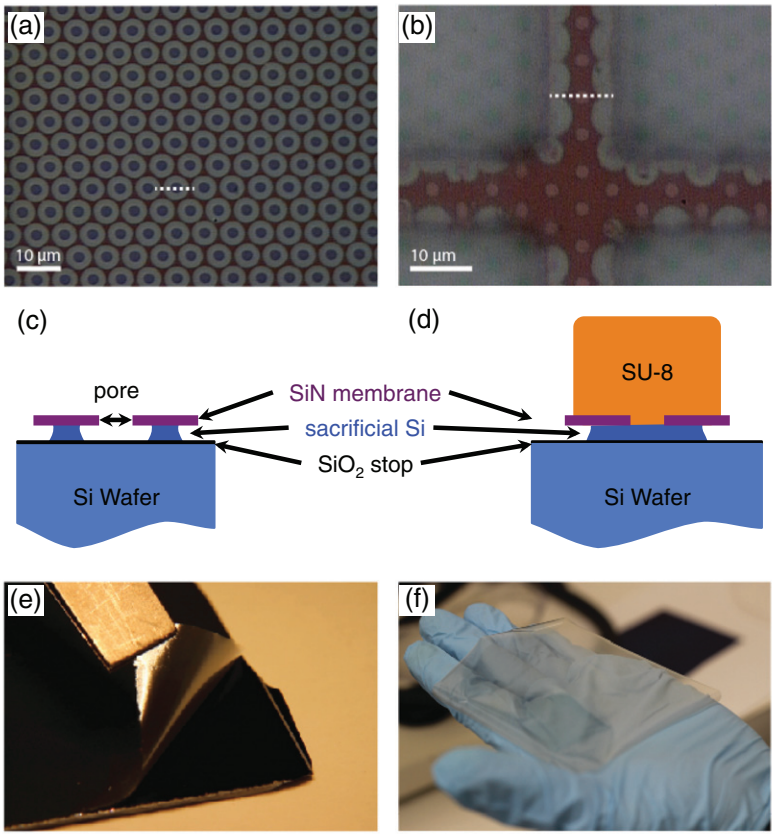

Figure 2. XeF_2 membrane lift-off. (*a*) Top down optical micrograph of the SiN membrane on the Si wafer after exposure to two XeF_2 pulses. Dark blue dots show the ø2 μm pores, the surrounding light gray rings show areas where the sacrificial silicon layer has been etched away, and the remaining red region shows the remaining silicon layer under the SiN film. (*b*) Higher magnification image of same sample showing a region of SU-8 scaffold. The scalloped light gray regions along the edges of the SU-8 features show where the sacrificial silicon has been etched. (*c*) Schematic representation of the cross-sectional view across a pore corresponding to the region highlighted with a dashed white line in (*a*). (*d*) Similar schematic for the region under an SU-8 scaffold feature corresponding to dashed white line in (*b*). (*e*) Photograph of the initial part of the lift-off for a 50 nm thick SiN membrane from a 7.5 × 10 cm silicon wafer section. Tweezers are used to lift the membrane starting at one corner. (*f*) Photograph of same membrane sample after lift-off.

as would be expected of a 50 nm thick film [30] (figures 2(*e*) and 3(*b*)). The presence of the 10 μm thick SU-8 scaffold on the backside does not result in any noticeable membrane pillowing or buckling under SEM. Figures 3(*c*) and (*d*) show scanning electron microscopy (SEM) images nanoporous SiN membranes that were obtained in some exploratory tests using the same etching method as used for the microporous membrane. One significant challenging aspect of the nanoporous membrane lift-off is in native oxide strip. Due to the hydrophobic nature of the nitride, wetting it with a BOE solution is more difficult. While it was possible to lift-off samples of the nanoporous membrane, it was observed that significantly more pulses of the XeF_2 etchant were necessary. This is likely an indication that the native oxide was not sufficiently stripped and will be the subject of future development by our group.

3.3. BOE lift-off

Lift-off using BOE in tandem with a silicon dioxide sacrificial layer was also explored. The reaction for this process is

$$6HF + SiO_2 \rightarrow H_2SiF_6 + 2H_2O. \quad (2)$$

Three different types of oxide were explored: thermal oxide, plasma-enhanced chemical vapor deposition (PE-CVD) of TEOS, and low-temperature reactive sputtering. The through-plane etch rates were measured to be 70 nm min^{-1}, 260 nm min^{-1} and 180 nm min^{-1} for thermal, PE-CVD and sputtered oxides, respectively. The etch rate of the SiN layer was measured in a control test to be 0.20 nm min^{-1}. Interestingly, it was found that the etch rates in the lateral, under-pore direction are roughly equivalent among the three oxide types at 190 nm min^{-1}. The similarity of horizontal etch rates likely indicates that mass transport of reactant and product species in the ~100 nm thick region under the SiN membrane that is defined by the sacrificial layer's thickness is dominating in the overall etch rate. The etch time for lift-off was observed to be 30–40 min, which agrees with that predicted for the longest etch distance (diagonal across SU-8 strut intersections or ~7 μm) divided by the average horizontal etch rate. Figures 4(*a*)–(*c*) show the fixtures that were used in the BOE lift-off etch and nanomembrane recovery once it was separated from the wafer substrate. Examples of the micro- and nano-porous membranes after lift-off are shown in figures 4(*a*) and (*b*), respectively. Because a significant amount of the SiN membrane is lost (10–20 nm)

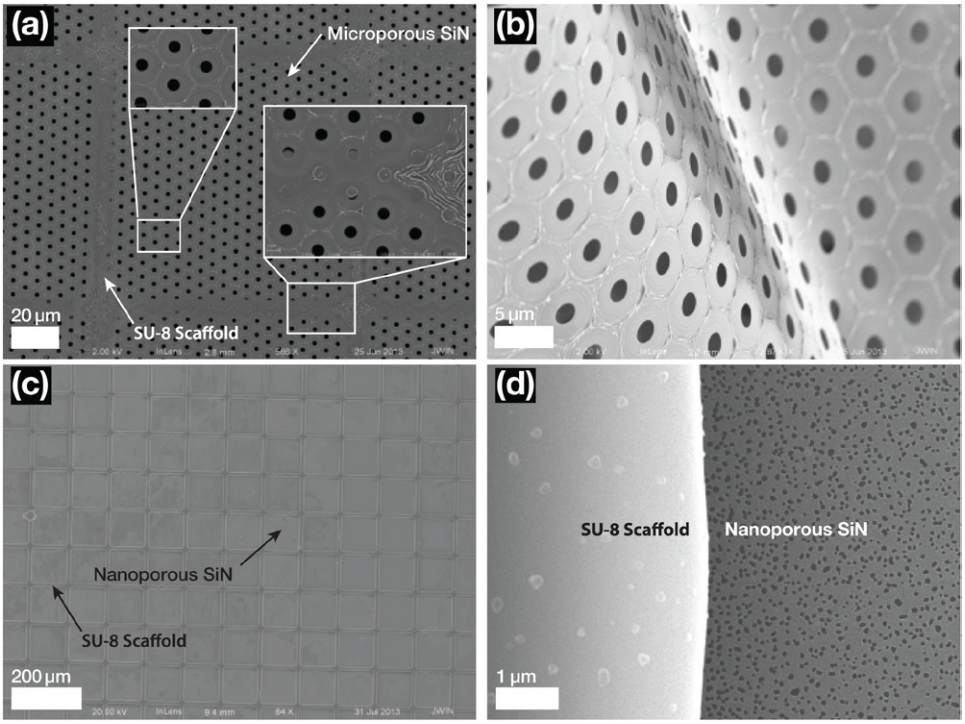

Figure 3. SEM micrographs of XeF_2 lift-off membranes. (*a*) Image of the bottom surface of a 50 nm thick microporous SiN membrane that had been in contact with the sacrificial silicon prior to a XeF_2 etch. The insets show evidence of the through-pore etch progress as a series of 'coffee ring' features. (*b*) Image of a free-standing lift-off membrane near an edge that was curling. This image shows the remarkable flexibility of the lifted-off membrane. (*c*) SEM image of a 50 nm thick nanoporous SiN membrane showing a fully intact membrane after lift-off. (*d*) High magnification image of the scaffold–membrane border on a nanoporous SiN membrane illustrating the absence of stress-induced wrinkling.

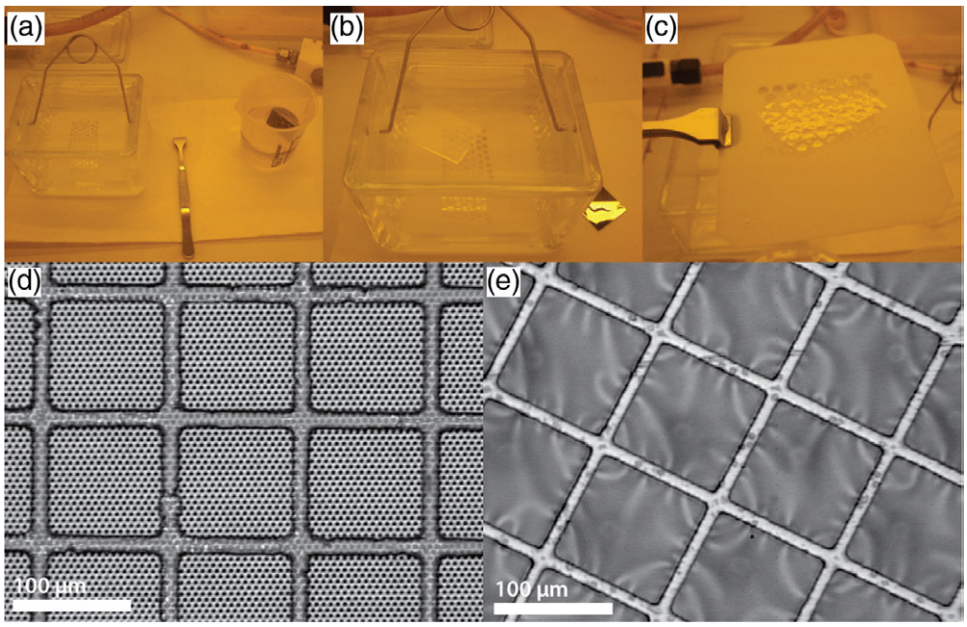

Figure 4. BOE membrane lift-off. (*a*) Beaker on right contains the wafer sample in the BOE etch, and water bath with membrane removal tray are shown on the left. (*b*) Lifted off membrane floating on surface of water bath following the through-pore etch (support wafer section is already removed from water bath). (*c*) Image of the membrane supported on the perforated plastic sieve used to remove the membrane from the water bath. Microporous (*d*) and nanoporous (*e*) SiN membranes floating on a water surface after BOE lift-off.

during the BOE etch, these nanomembranes are generally not as robust as the ones produced in the dry etch (XeF_2) process. This could be mitigated in part by depositing a thicker SiN layer, but there is also the consideration that the pore size will increase as the SiN is etched during the BOE process. As mentioned above, the motivation for exploring the BOE method is to enable potential future development of a lift-off method for a silicon membrane such as the pnc-Si.

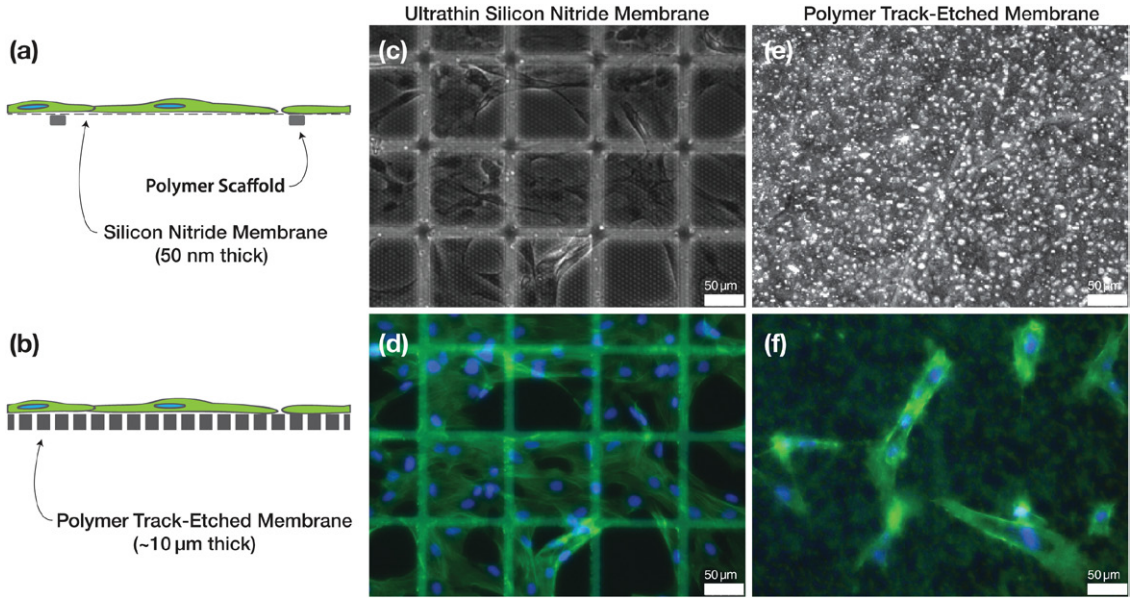

Figure 5. ADSCs were cultured on microporous membranes and imaged on an inverted microscope. Cross-sectional illustrations of cells grown on ultrathin SiN membranes (*a*) and conventional TE cell culture membranes (*b*) are drawn approximately to scale. (*c*) Edges of ADSCs are easily discerned in phase contrast on microporous lift-off SiN membranes. (*d*) Fluorescently labeled actin filaments are visible when imaging through ultrathin SiN membranes. (*e*) Conventional TE membranes prevent imaging in phase contrast due to scattering. (*f*) Likewise, fluorescence imaging through TE membranes results in blurred features and significant background after staining.

3.4. Cell culture on lift-off membranes

One application domain that would be enhanced by larger area nanomembranes is cell culture. Efforts to differentiate adult and embryonic stem cells has emphasized the microenvironment and cues from neighboring cells [31, 32]. In our recent work inducing ADSCs toward an endothelial lineage, we showed that differentiation on porous membranes in close proximity to human endothelial cells is necessary [18]. Here we find that ADSCs adhere, spread and proliferate normally on lift-off SiN membranes with SU-8 scaffolding, with no adverse affects as a result of the lift-off process. We cultured the cells in a custom designed silicone gasket device with a 6.5 mm circular lift-off membrane, which is comparable in size to standard 24-well commercial membrane inserts (online supplemental figure S2 (stacks.iop.org/JMM/25/015011)). While polymer TE membranes have been used for some transmembrane co-culture studies, they are dramatically thicker than Si-based membranes (figures 5(*a*) and (*b*)). Ultrathin SiN membranes are relatively transparent, enabling high quality phase contrast and fluorescence imaging of subcellular structures (figures 5(*c*) and (*d*)). Polymer TE membranes, however, have significant scattering in phase contrast and an increased fluorescence background signal after staining (figures 5(*e*) and (*f*)). Improved imaging with ultrathin SiN membranes enables live imaging of differentiating cells in addition to providing a more permeable physical support. Lift-off of SiN membranes enables for the first time, nanomembrane integration into standard-size cell culture plates.

While the scaffold geometry in this work was optimized for developing lift-off techniques, it is also feasible to create polymeric scaffolds for the purpose of capturing and manipulating individual cells or small colonies. Single cell or colony analysis offers insights into heterogeneity and variability during stem cell differentiation and drug response [33, 34]. Prior studies on non-porous substrates have used a variety of materials including SU-8, polydimethyl siloxane (PDMS), and polyethylene glycol (PEG) to fabricate gratings or microwells to culture cells [35]. These structures typically have slightly taller walls than the lift-off scaffold to facilitate capture and retention of cells during loading. The lateral dimensions of the microwells vary depending on the application, but are on the same order of magnitude as the lift-off scaffold presented here. Future work on lift-off could incorporate scaffold optimizations to create microwells on a membrane. The porous membrane floor would enable communication across the membrane in a co-culture arrangement that would be applicable for stem cell differentiation and other cellular paracrine signaling studies.

4. Conclusion

In summary, a novel approach is described for fabricating 50 nm thick, microporous and nanoporous SiN membranes with free-standing areas of many square centimeters. Our approach involves first patterning a microscopic scale support scaffold from a negative resist polymer followed by a through-pore etch of an underlying sacrificial layer to enable release or lift-off. The efficacy of lift-off was demonstrated with two etch methods: XeF_2 etch of a sacrificial poly-silicon layer and BOE etch of a sacrificial silicon dioxide layer. In addition to creating ultrathin membranes of SiN, these two etch techniques could be used in lift-off of pure silicon membranes using BOE and silicon dioxide membranes using XeF_2. The utility of lift-off membranes in cell culture was demonstrated

through culture of ADSCs. This represents the first time that ultrathin porous silicon-based membranes have been fabricated at the scale of conventional cell culture substrates. Stem cell differentiation at this scale is generally necessary for clinical and therapeutic uses [19]. In future studies, it would be possible to create thicker scaffolds of prescribed geometries for single cell or small colony heterogeneity studies during differentiation. The lift-off membrane's ability to be manually handled and remarkable flexibility also offers great promise for nanomembrane use in a range of other applications including portable hemodialysis [14].

Acknowledgments

The authors would like to thank the staff at RIT's Semiconductor and Microsystems Fabrication Laboratory for training and assistance with tool optimization. This work was funded in part by Gleason Family Foundation. A corporate start-up, SiMPore Inc., participated in this work. SiMPore is working to commercialize ultrathin silicon membranes. TRG and CCS are co-founders of SiMPore. JJM and JSD are current employees of SiMPore.

References

[1] Han J, Fu J and Schoch R B 2008 Molecular sieving using nanofilters: past, present and future *Lab Chip* **8** 23–33
[2] Snyder J L, Clark A, Fang D Z, Gaborski T R, Striemer C C, Fauchet P M and McGrath J L 2011 An experimental and theoretical analysis of molecular separations by diffusion through ultrathin nanoporous membranes *J. Membrane Sci.* **369** 119–29
[3] Conlisk A T, Datta S, Fissell W H and Roy S 2009 Biomolecular transport through hemofiltration membranes *Ann. Biomed. Eng.* **37** 722–36
[4] Jeon G, Yang S Y and Kim J K 2012 Functional nanoporous membranes for drug delivery *J. Mater. Chem.* **22** 14814–34
[5] Haque F, Li J, Wu H-C, Liang X-J and Guo P 2013 Solid-state and biological nanopore for real-time sensing of single chemical and sequencing of DNA *Nano Today* **8** 56–74
[6] Kim E, Xiong H, Striemer C C, Fang D Z, Fauchet P M, McGrath J L and Amemiya S 2008 A structure–permeability relationship of ultrathin nanoporous silicon membrane: a comparison with the nuclear envelope *J. Am. Chem. Soc.* **130** 4230–1
[7] Siwy Z, Kosińska I, Fuliński A and Martin C 2005 Asymmetric diffusion through synthetic nanopores *Phys. Rev. Lett.* **94** 048102
[8] Qi C, Striemer C C, Gaborski T R, McGrath J L and Fauchet P M 2014 Highly porous silicon membranes fabricated from silicon nitride/silicon stacks *Small* **10** 2946–53
[9] Agrawal A A, Nehilla B J, Reisig K V, Gaborski T R, Fang D Z, Striemer C C, Fauchet P M and McGrath J L 2010 Porous nanocrystalline silicon membranes as highly permeable and molecularly thin substrates for cell culture *Biomaterials* **31** 5408–17
[10] Striemer C C, Gaborski T R, McGrath J L and Fauchet P M 2007 Charge- and size-based separation of macromolecules using ultrathin silicon membranes *Nature* **445** 749–53
[11] Gaborski T R, Snyder J L, Striemer C C, Fang D Z, Hoffman M, Fauchet P M and McGrath J L 2010 High-performance separation of nanoparticles with ultrathin porous nanocrystalline silicon membranes *ACS Nano* **4** 6973–81
[12] Snyder J L, Getpreecharsawas J, Fang D Z, Gaborski T R, Striemer C C, Fauchet P M, Borkholder D A and McGrath J L 2013 High-performance, low-voltage electroosmotic pumps with molecularly thin silicon nanomembranes *Proc. Natl Acad. Sci. USA* **110** 18425–30
[13] Chung H H, Chan C K, Khire T S, Marsh G A, Clark A, Waugh R E and McGrath J L 2014 Highly permeable silicon membranes for shear free chemotaxis and rapid cell labeling *Lab Chip* **14** 2456–68
[14] Johnson D G, Khire T S, Lyubarskaya Y L, Smith K J P, Desormeaux J-P S, Taylor J G, Gaborski T R, Shestopalov A A, Striemer C C and McGrath J L 2013 Ultrathin silicon membranes for wearable dialysis *Adv. Chronic Kidney Dis.* **20** 508–15
[15] Desormeaux J-P S, Winans J, Wayson S E, Gaborski T R, Khire T S, Striemer C C and McGrath J L 2014 Nanoporous silicon nitride membranes fabricated from porous nanocrystalline silicon templates *Nanoscale* **6** 10798–805
[16] Harris S G and Shuler M L 2003 Growth of endothelial cells on microfabricated silicon nitride membranes for an *in vitro* model of the blood–brain barrier *Biotechnol. Bioprocess Eng.* **8** 246–51
[17] Ma S H, Lepak L A, Hussain R J, Shain W and Shuler M L 2005 An endothelial and astrocyte co-culture model of the blood–brain barrier utilizing an ultra-thin, nanofabricated silicon nitride membrane *Lab Chip* **5** 74–85
[18] Mazzocchi A, Man A, Desormeaux J-P S and Gaborski T R 2014 Physical separation of endothelial and adipose-derived stem cells using a porous nanomembrane promotes differentiation and cell reorganization *Cell. Mol. Bioeng.* **7** 369–78
[19] Reckhenrich A K, Kirsch B M, Wahl E A, Schenck T L, Rezaeian F, Harder Y, Foehr P, Machens H-G and Egaña J T 2014 Surgical sutures filled with adipose-derived stem cells promote wound healing *PLoS One* **9** e91169
[20] Tong H D, Jansen H V, Gadgil V J, Bostan C G, Berenschot E, van Rijn C J M and Elwenspoek M 2004 Silicon nitride nanosieve membrane *Nano Lett.* **4** 283–7
[21] Kuiper S, Van Rijn C, Nijdam W and Elwenspoek M C 1998 Development and applications of very high flux microfiltration membranes *J. Membrane Sci.* **150** 1–8
[22] Halverson R M, MacIntyre M W and Motsiff W T 1982 The mechanism of single-step liftoff with chlorobenzene in a diazo-type resist *IBM J. Res. Dev.* **26** 590–5
[23] Collins G G and Halsted C W 1982 Process control of the chlorobenzene single-step liftoff process with a diazo-type resist *IBM J. Res. Dev.* **26** 596–604
[24] Bustillo J M, Howe R T and Muller R S 1998 Surface micromachining for microelectromechanical systems *Proc. IEEE* **86** 1552–674
[25] French P J and Sarro P M 1998 Surface versus bulk micromachining: the contest for suitable applications *J. Micromech. Microeng.* **8** 45
[26] Ghodssi R and Lin P 2011 *MEMS Materials and Processes Handbook* (Berlin: Springer)
[27] Williams K R, Gupta K and Wasilik M 2003 Etch rates for micromachining processing: II *J. Microelectromech. Syst.* **12** 761–78
[28] Edwards R L, Coles G and Sharpe W N Jr 2004 Comparison of tensile and bulge tests for thin-film silicon nitride *Exp. Mech.* **44** 49–54
[29] Chuang W H, Luger T, Fettig R K and Ghodssi R 2004 Mechanical property characterization of LPCVD silicon nitride thin films at cryogenic temperatures *J. Microelectromech. Syst.* **13** 870–9
[30] Rogers J A, Lagally M G and Nuzzo R G 2011 Synthesis, assembly and applications of semiconductor nanomembranes *Nature* **477** 45–53

[31] Bunnell B A, Flatt M, Gagliardi C, Patel B and Ripoll C 2008 Adipose-derived stem cells: isolation, expansion and differentiation *Methods* **45** 115–20
[32] Merfeld-Clauss S, Gollahalli N, March K L and Traktuev D O 2010 Adipose tissue progenitor cells directly interact with endothelial cells to induce vascular network formation *Tissue Eng.* A **16** 2953–66
[33] Di Carlo D and Lee L P 2006 Dynamic single-cell analysis for quantitative biology *Anal. Chem.* **78** 7918–25
[34] Charnley M, Textor M, Khademhosseini A and Lutolf M P 2009 Integration column: microwell arrays for mammalian cell culture *Integr. Biol. (Camb.)* **1** 625–34
[35] Lindström S and Andersson-Svahn H 2010 Overview of single-cell analyses: microdevices and applications *Lab Chip* **10** 3363–72